

# Spatial Approximation of Terrestrial Laser Scanner Profiles by Considering Observations with Stochastic Information

Hamza ALKHATIB, Claudius SCHMITT and Ingo NEUMANN, Germany

**Key words:** Terrestrial Laser Scanning, Free-form curves, Monte Carlo Methods, B-Splines

## SUMMARY

The monitoring of structure works, as bridges, tunnels and embankment dams, is in various engineering disciplines an important task. The main goal of this monitoring includes the evaluation of their life cycle, and the developing of concepts to increase their expected life as well. The geodetic task, hereby, is to deliver independent concepts for both, the measurement metrology and evaluation methods in order to provide the deflection with or without load. Deformations in structure works, to be monitored, could be determined frequently by means of kinematic terrestrial laser scanning (k-TLS). In an interdisciplinary project between the Geodetic Institute and the Institute of Solid Construction (both at the University of Hanover), a prestressed concrete bridge has been investigated. As contactless surveying approach, the k-TLS was used to measure the deflection of the bridge construction. In further research works, the nonlinear profiles have been spatially approximated using approaches of free-form curves, B-Splines. These show much better results compared to the section wise block mean values around discrete profile positions. Statistical hypothesis tests have shown, that resulting residuals of the free-form curves approximation still contain random and systematic effects, which arise from the sensor itself, from the surface structure of the object and model and from the environment. In many cases, the uncertainty of output parameters is computed by assuming that the distribution function of the measurements is normally distributed with zero mean and equally weighted and stochastically independent variance-covariance-matrix. This assumption may be unjustified and the uncertainty of the output quantities (parameter and residuals) so determined may be incorrect. One tool to deal with random and systematic uncertainties of the input parameters and the resulting mixed-distribution of the output quantities is given through the Monte Carlo techniques. This study deals with two main topics: the refined simulation of different configurations by taking different covariance structures of the input parameters (2-D coordinates of TLS profile), and the statistical analysis of the resulting residuals in order to improve the physical observation models.

# Spatial Approximation of Terrestrial Laser Scanner Profiles by Considering Observations with Stochastic Information

Hamza ALKHATIB, Claudius SCHMITT and Ingo NEUMANN, Germany

## 1. INTRODUCTION

The sequential scanning of surface structures is getting more and more a standard metrology in engineering geodesy. Because of the enormous amount of single points in a point cloud classical geodetic point based analysis are not sufficient enough to catch the entire information of this point cloud. For a surface based metrology a surface based analysis of the data is necessary to observe the whole potential of the measured data. Especially terrestrial laser scanner (TLS) are such sensors, which produces up to one million points per second in 1D, 2D or 3D coordinates. Within this high measuring rate not only surfaces can be efficiently mapped in a static environment the focus lies also on kinematic application. Measuring the deflection of a concrete bridge during the impact of traffic load from trucks and cars are an example of kinematic applications, whereby the TLS station is immovable and deployed in the 2D profile mode which is than further mentioned as k-TLS. One of these first experiments in relation to bridges are shown in (Kutterer et al. 2009), Paffenholz et al. (2008) and in Liebig et al. (2011). The results of this experiment are time series of 2D profile lines discretized by sequentially measured 2D single point. To detect the deflection of the bridge from the profiles they need to be spatially approximated to increase the accuracy. The easiest way to accomplish this is to process block wise mean values for the deflection as in (e. g. Kutterer et al. 2009 and Liebig et al. 2011). As shown in (Schmitt et al. 2013, Neuner et al. 2013) the model of mean values is not accurate enough by nonlinear surfaces. Instead, the model of a free form curve adapts the nonlinear structure much better to consequently improve the accuracy of the approximated deflection. So that the deflection of up to 1.5 mm can significantly be extracted (e. g. Schmitt et al. 2013, Neuner et al. 2013). In the past the stochastic information in both models, the block wise mean values and the free form curves, of the single points were neglected and reduced to the identity matrix. In this paper the influence of the stochastic model of the observations at the free form curve approximation with B-Splines is shown, by the use of a priory variance-covariance information calculated with classical propagation of uncertainty and Monte Carlo modelling methods to reduce the systematic effects in the residuals.

The paper is organized as follows: First we will describe the functional approximation by means of the free-form curves. In Section 3 describes the stochastic model and the measurement uncertainties in the context of GUM. Two different approaches will be discussed: the classical approach using the variance covariance propagation and the Monte Carlo approach (MC GUM). The application example, monitoring of a bridge, to kinematic TLS is given and discussed in the Section 4. Section 5 summarizes the results.

## 2. FUNKTIONAL APPROXIMATION BY MEANS OF FREE-FORM CURVES

For the spatial approximation of the profile data free-form curves in terms of B-Splines are used as described in (Piegel L., Tiller W. 1997, De Boor 1989). B-splines in a global approximation can model the data with the focus on local characteristics by low degree of the

piecewise polynomial functions. In the past, the B-Splines were approximated in a least squares sense without any stochastic information for the observations (2D Cartesian coordinates). Within this study, B-spline curve approximation were used regarded to their stochastic information for the observations, shown in chapter 3.

Based on the expected deflection and the expected shape of the bridge structure, more detailed described in 4.1, the functionality of the B-spline is sufficient enough for this application. In case of circular structures, the B-spline needs to be extended to non-uniform rational B-spline (NURBS) to reproduce the geometry without numerical defects.

B-splines are special for their original use. They were first developed for virtual construction and design and not for approximation domain. That's why it is not as comfortable to use them in least squares within the optimization of all its parameters in a linear estimation, compared to polynomial approaches (e.g. Heunecke et al. 2013). Some of the parameters were assumed in further experiments and chosen as best in this application, like the degree  $p$  and the number of basis functions  $n$ .

The functional model is described by the degree and it's basis functions  $N$ , defined by the Bernstein polynomial associated with the internal knot vector  $U$ , with number  $m$ . Thereby  $uk_h$  is a specific position on the B-spline and the control points  $P$  (in three dimensional Cartesian coordinates), as the unknowns, to

$$C(uk_h) = \sum_{i=1}^{n+1} N_{i,p}(uk_h)P_i \quad (1)$$

$$U\{0_{1,\dots,p+1}, a_{p+2}, \dots, a_{m-p-2}, 1_{m-p-1,\dots,m}\}$$

with  $0 < a < 1$ : variable internal knots and the relation between the internal knots, the number of the basis functions and the degree of the piecewise polynomial function to

$$n = m - p - 1. \quad (2)$$

The measured TLS points  $Q$ , the observations in 2D Cartesian coordinates, with number  $h$ , and its parametric equivalent B-Spline value ( $uk_h$ ). The result of  $C(uk_h)$  at  $0 < uk < 1$ , are then approximated in a least squares sense by minimizing of (Piegel L., Tiller W. 1997)

$$\sum_{k=1}^h |Q_h - C(uk_h)|^2 \rightarrow \min. \quad (3)$$

to get estimated control points  $\bar{P}$ , the a priory unknowns, with the restriction that the B-spline pass through the first and last measured point and the slope of the tangent at the first and last point are the equivalent straight lines of the control net, e. g. Figure , respectively from  $P_1 \rightarrow P_2$  and  $P_n \rightarrow P_{n+1}$  . Therefore the measured points need to be transformed into parameter values  $k$  , which is done by the normalized summation of the distance between the points from the beginning. To get a positive definite and well-conditioned normal equation system the intern knots  $a$  of the internal knot vector  $U$  are computed from the  $uk$ 's (De Boor 1989):

$$a_{p+j+1} = (1 - \alpha)uk_l + \alpha uk_{l+1} \quad (4)$$

with  $j = 1, \dots, n - p - 1$ ;  $l = \text{integer}(jd)$ ;  $\alpha = jd - l$  and  $d = \frac{m}{n-p}$ .

The basis function is dependent of the used Grad  $p$  of the function. The multiplication of the design matrix  $\mathbf{A}$  and the unknown control points  $\mathbf{u}$  is equal to the curve  $C$  of the free form curve:

$$C(\mathbf{x}) = \mathbf{A} \cdot \mathbf{u} \text{ mit } \mathbf{u} = \begin{bmatrix} P_1 \\ P_2 \\ \vdots \\ P_n \end{bmatrix}, \mathbf{A} = \begin{bmatrix} N_{1,p}(x_1) & \cdots & N_{n,p}(x_1) \\ \vdots & \vdots & \vdots \\ N_{1,p}(x_m) & \cdots & N_{n,p}(x_m) \end{bmatrix}. \quad (5)$$

The full rank design matrix  $\mathbf{A}$  contains all the values of the basis functionn in the individuall postions of the x-axis.

### 3. STOCHASTIC MODELLING WITH MONTE CARLO TECHNIQUES

The assessment and propagation of uncertainty is an important issue in all disciplines which rely on measurements such as geodesy. In a refined model the observations are related to some basic influence parameters which depend – in case of TLS – on the scanning device, on the scanning process and on the environmental conditions. It is common practice to model observable quantities as random vectors. In the standard case such random quantities are assumed as normally distributed; from this it follows their stochastic properties are uniquely determined by the expectation vector and the variance-covariance matrix.

The ‘‘Guide to the Expression of Uncertainty in Measurement (GUM)’’ is a standard reference in uncertainty modeling in engineering and mathematical sciences, cf. ISO (1995; ISO, 2007). GUM groups the occurring uncertain quantities into ‘‘Type A’’ and ‘‘Type B’’. Uncertainties of ‘‘Type A’’ are determined with the classical statistical methods, while ‘‘Type B’’ is subject to other uncertainties which are obtained by experience and knowledge about an instrument or a measurement process. Whereas the uncertainties of the quantities of ‘‘Type A’’ can be estimated based on repeated measurement of the quantity of interest, the estimated uncertainties of the quantities of ‘‘Type B’’ are based on expert knowledge, e.g., the technical knowledge about an instrumental error source. GUM defines an output quantity  $y$  as a function of input quantities  $Z$ . The input quantities can be considered as influence parameters which, e.g., can be relevant in pre-processing steps:

$$\mathbf{Y} = f(Z_1, Z_2, \dots, Z_n) = f(\mathbf{Z}) \quad (6)$$

Here  $\mathbf{Y}$  represents a random output quantity vector and  $Z_1, Z_2, \dots, Z_n$  are the  $n$  random inputs. In case of a different distribution the probability density function has to be formulated explicitly. For numerical calculations the values of all model parameters have to be quantified. For this purpose dedicated experiments can be performed; long-term experience or expert knowledge can also be used.

If the observations are processed and analyzed by mathematical means, the uncertainty of the derived quantities has to be calculated as well. In case of non-linear functional relations a linearization is typically applied. Then, the propagation of expectation vectors and variance-

covariance matrices in linear mappings is straightforward; the latter is known as the law of error propagation or variance propagation, respectively (Alkhatib et al. 2009, Kutterer et al 2010).

$$u^2(\mathbf{Y}) = \mathbf{F}\Sigma_{ZZ}\mathbf{F}^T \quad (7)$$

where  $\mathbf{F}$  contains the partial derivatives  $\mathbf{Y} = f(\mathbf{Z})$  with respect to  $p_1, p_2, \dots, p_n$  that is

$$\mathbf{F} = \begin{bmatrix} \frac{\partial f_1}{\partial z_1} & \dots & \frac{\partial f_1}{\partial z_n} \\ \vdots & \ddots & \vdots \\ \frac{\partial f_u}{\partial z_1} & \dots & \frac{\partial f_u}{\partial z_n} \end{bmatrix} \quad (8)$$

and  $\Sigma_{ZZ}$  is the uncertainty matrix of the input quantities  $\mathbf{Z}$ .

For complete distributions the convolution of probability densities is required; moments such as the expectation vector or the variance-covariance matrix are then derived using the well-known integral relations. Such approaches are also used in international standards (ISO, 1995; ISO, 2007).

In general, the functional relations between the basic influence parameters, the observations and the parameters of interest are non-linear, and the normal distribution is not the adequate probability density function. In such a case, Monte-Carlo simulation is a suitable way to approximately derive the stochastic properties of the quantities of interest (output quantities). It is assumed that the functional model is completely formulated relating the output quantities with the input quantities – the observations and the basic influence parameters, respectively. It is further assumed that the probability densities of the considered input quantities are a priori known. Then, a sample vector of the input quantities can be drawn repeatedly using random number generators. For each input sample vector, the corresponding values of the output quantities are calculated by using the corresponding functional relation. The set of output sample vectors yields an empirical distribution, which can be used to approximate the correct random distribution of the output quantities. All required measures (expectation values, variances and covariances) as well as higher order central moments such as skewness and kurtosis can then be derived. A detailed description of the algorithms to compute the required moments can be found in (Alkhatib et al. 2009, in Alkhatib and Kutterer 2013).

Obviously, this approach is straightforward. (Koch 2008) discusses Monte-Carlo simulation in case of TLS uncertainty assessment. (Alkhatib et al. 2009) apply it to k-TLS vertical profile scans and they merge it with a set-theoretical approach based on fuzzy sets. In Alkhatib and Kutterer (2013) pure Monte-Carlo simulation is considered but it is extended to the discussion of the properties of the derived time series and of their validation using real k-TLS observation data.

#### 4. APPLICATION TO K-TLS

In this section a short numerical example for the comparison of the two approaches from Section 2 and 3 is presented. The aim of the application is to detect the vertical displacements of a bridge under load, e.g., due to car traffic or train crossings. For this reason, a laserscanner

of type Zoller+Fröhlich Imager 5006 scanner was placed beneath the bridge which is located near Hanover.

#### 4.1 Object and Setup

In an interdisciplinary project based on “Application of life cycle concepts to civil engineering structures” described more detailed in (NTH-BAU 2010, Hansen et al. 2012), at the University of Hannover, a prestressed concrete bridge near Hannover was investigated. The geodetic part was to provide an independent metrology to compute strain values derived from the approximated deflections. (This paper focuses on the improvements of getting the deflection values.) The structure is built in 1975 with one box beam and side extensions on both sides. The bridge is an overpassing over several tracks and streets and connects the city with the adjoining villages. It’s total width measures 14 m and the width of the two mutual lanes is 10 m. The total length is 404.55 m segmented into 13 sections. In section three denoted as MQ3, see Figure 1, the contactless TLS metrology for this study is installed.

The terrestrial laser scanner can detect the geometry changes over time. In this experiment, the phase comparison based TLS from ZÖLLER+FRÖHLICH, Imager 5006, with an RMS value for distance measurements (20% reflectivity) of 0.7 mm is used (ZÖLLER+FRÖHLICH 2007). This measurement is accurate enough to detect deflections caused by truck load between 0.5 mm to 1.5 mm associated with the spatial approximation, approved by (e. g. Schmitt et al. 2013, Neuner et al. 2013) and is shown by the results later on. For the measurements the TLS is positioned under the middle of the bridge segment, and aligned along the main axis of the bridge (e. g. Figure 2, red dotted line) so that the outside bottom of the box beam is contactless scanned with a shortest distance of ~4.7 m.

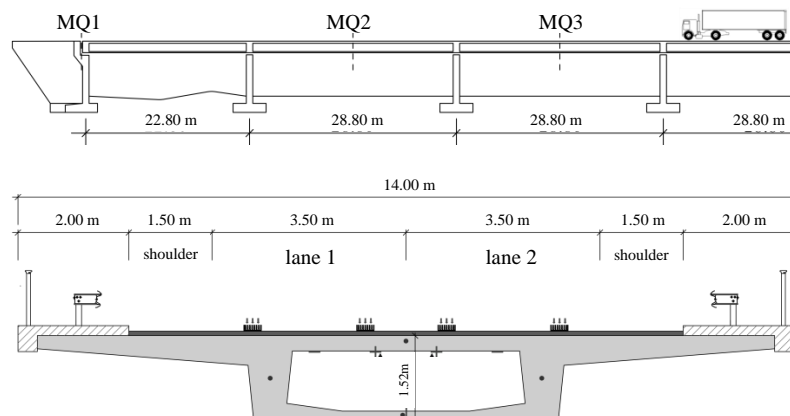


Figure 1: Bridge structure longitudinal section (above), cross section (below)

As measuring type the profile mode was chosen with a sampling interval of 0.08 seconds per profile, i.e. 12.5 Hz sampling rate. The point sampling rate was 500 000 points per second and results into ~13000 points in each profile at the box beam. These parameters are figured out best in various pre experiments (e. g. Schmitt et al. 2013, Neuner et al. 2013). The chosen scanner parameters permit an adequate ratio between accuracy and measuring frequency.

With its high sampling rate of 12.5 Hz up to 50 Hz and the possibility of synchronization with other sensors it is predestinated for time continuously measurements.

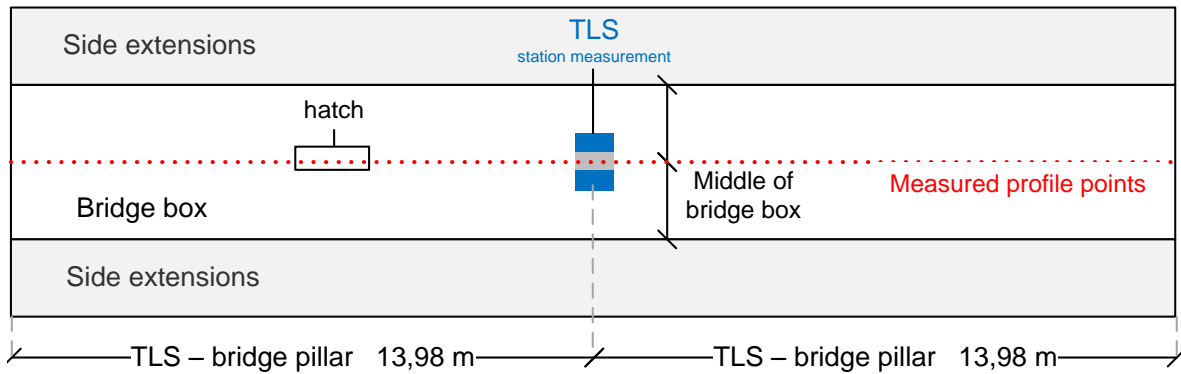


Figure 2: Layout of the measurement setup - bridge section at MQ3, TLS station (blue-gray) and the profile direction (red dotted line)

#### 4.2 Derivation of k-TLS Profiles uncertainties for the measurements influence factors

For the simulations, the functional model described in Kutterer et al. (2010) and in Alkhatib and Kutterer (2013) was used as a basis. In this previous study, seven uncertainty components were modeled. However, during various simulation runs this number could be reduced to a subset of only three to four essential parameters which induce uncertainty. The remaining parameters are: the observed distance  $d$  between laser scanner and object point which induces a constant and a distance-proportional effect, the observed zenith angle  $\zeta_0$  with a constant angular effect, and the discretization term  $\Delta\zeta$  which is induced by the angular increment of the vertical servo-motor. The first three parameters are considered as normally distributed whereas the last parameter is assumed as uniformly distributed. The mathematical model for the derivation of the coordinate  $z$  and  $y$  (the output quantities vector, see Eq. 5) is straightforward:

$$z = d \cos \zeta \quad \text{and} \quad y = d \sin \zeta \quad (9)$$

with  $d \sim N(m_d, \sigma_d^2)$  and  $\zeta_0 \sim N(m_{\zeta_0}, \sigma_{\zeta_0}^2)$  and  $\Delta\zeta \sim U(\Delta\zeta_l, \Delta\zeta_u)$ . The symbols  $m$  and  $\sigma$  denote the expectation value and the variance of the random variable, respectively; the uniform distribution is defined by the lower bound  $\Delta\zeta_l$  and the upper bound  $\Delta\zeta_u$  of the interval with positive values of the density function. Note that the effect of the angle of incidence on the uncertainty of the profile points was not considered in this study although its presence is well-known. This is due to the strong correlation of this effect with the distance-proportional effect in the considered observation configuration. More refined configurations and uncertainty models will be discussed in a following study. In this study, four uncertainty components were modeled:

- Uncertainty of the distance ( $Z_1$ ) and their additional constant.
- Distance depending term for the uncertainty of the distance measurement  $Z_2$
- Uncertainty of the zenith angle ( $Z_3$ )
- Vertical resolution for the zenith angle (the step width of the motor) ( $Z_4$ )

The uncertainties and the power density function (pdf) for the input quantities  $Z_1$  are given in

Table 1. A detailed description of the used stochastic model can be found in Alkhatib and Kutterer (2013).

Table 1: Uncertainty for input quantities models (type of probability densities and numerical values of the standard deviations).

| Input quantity $p_i$   | Error component | Power density function       | PDF Type    | Num. value (std. dev.) |
|------------------------|-----------------|------------------------------|-------------|------------------------|
| Distance: constant     | random          | $N(m_{Z_1}, \sigma_{Z_1}^2)$ | Normal      | 0.3 mm                 |
| Distance: proportional | systematic      | $N(m_{Z_1}, \sigma_{Z_1}^2)$ | Normal      | 30 ppm                 |
| Zenith angle           | random          | $N(m_{Z_3}, \sigma_{Z_3}^2)$ | Normal      | 5 mgon                 |
| Vertical increment     | random          | $U(Z_{7l}, Z_{7u})$          | Rectangular | 10 mgon                |

In the following, the results of the approximation given in Section 2 and 3 are shown. For the setup of the stochastic model, the classical GUM and Monte-Carlo simulation. For the last approach, 100.000 samples were drawn for each random quantity; the obtained values were processed according to the model described in Eq. (7).

### 4.3 Results

The parameters of the B-spline for the approximation are chosen as three for the degree and 21 for the number of control points. This parameters show the best result in the least squares within a model selection process out of 10 datasets with each having 3000 to 4000 profiles (Schmitt et al. 2013). Through one profile a section of ~14m, -7 m to +7 m related to the scanner station is used. The ~13000 measured points of each profile are approximated by the B-splines, e. g. 4, with the depicted TLS points (green), the estimated control points (red), and the B-spline (blue). As shown in (Schmitt et al. 2013, Neuner et al. 2013) the B-spline demonstrates reliable and accurate results for the spatial approximation. In Figure 3, the observations are assumed to be stochastically independent and have identical variances.

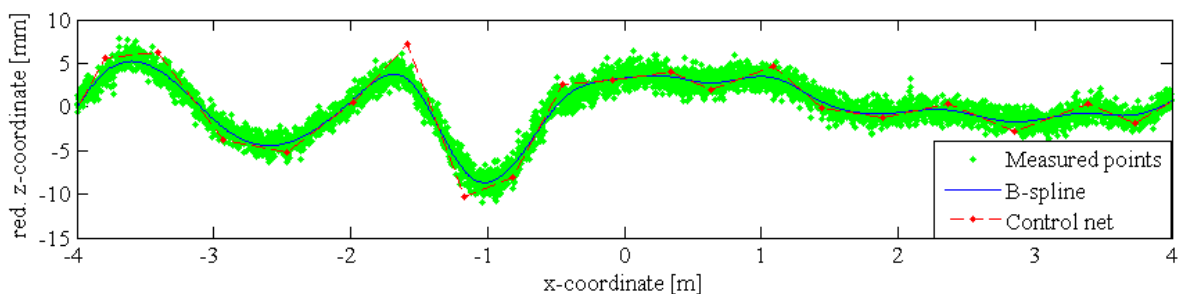


Figure 3: Profile approximation exemplified by B-spline with stochastically independent identical variances for the observations

In order to compute the Variance Covariance matrix (VCM) for observations (here y- and z-



coordinates), two different approaches (described in Section 3) are applied: The propagation process of the uncertainties using GUM approach and using Monte Carlo simulation. Figure 4 shows the resulting uncertainty only for the z-coordinate. As we can clearly see, the computed uncertainties differs mainly at the position  $y = 0$ , about 1,1 mm, and decreases in both directions (left and right). The computed uncertainty using classical GUM are more homogeneously and leads in average to pessimistic uncertainties compared to the MC approach. The maximal

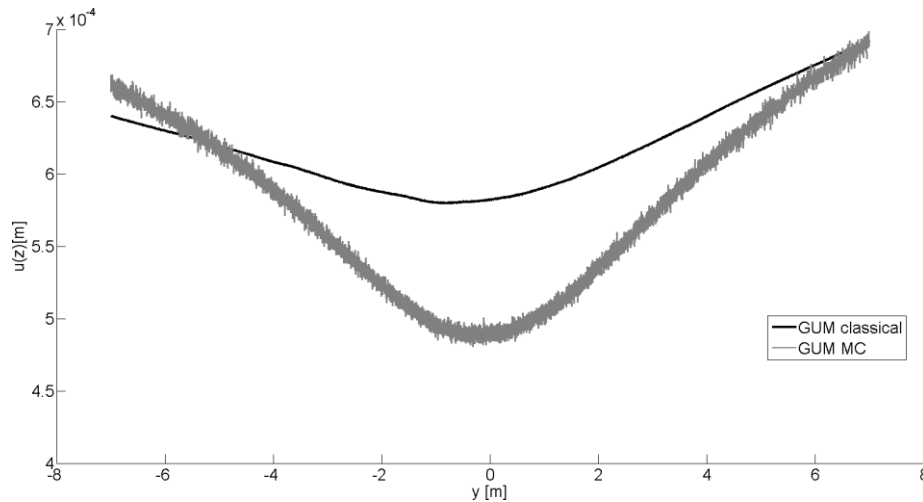


Figure 4: Comparison between computed uncertainties using classical GUM (black) and Monte Carlo GUM (gray).

For the GUM MC approach, 100.000 samples were drawn for each random quantity according to the Tab. 1. Looking at the standard deviations shown in Figure 5, the distance-proportional effect on the standard deviations of the representative profile points is obvious. Moreover, the square-root law  $\bar{\sigma} = \sigma_z / \sqrt{n}$  for the standard deviation of the mean value  $\bar{z}$  with respect to the standard deviation of the single values by the number  $n$  of sample values can clearly be seen. In addition, the skewness in Figure 6 is insignificant. The deviation of the normal distribution lies in the kurtosis. It is clearly violated in Figure 5. Note that for a rigorous mathematical assessment this discussion has to be referred to suitable hypothesis tests; however, the tendency is clear. Due to the convolution of two different probability distributions – normal and uniform, respectively – the resulting distribution is not a normal distribution. Moreover, the kurtosis values decrease from 3 (which is valid for observations directly in vertical direction and which does not contradict to the normal distribution assumption) to about 2,8 in a horizontal distance of about 0. There are two effects which superpose each other: one from the uniform distribution and the other from the (non-linear) cosine and sine function. In case of increasing the class width, the effect on the kurtosis is significantly mitigated – possibly due to the central limit theorem of probability theory.

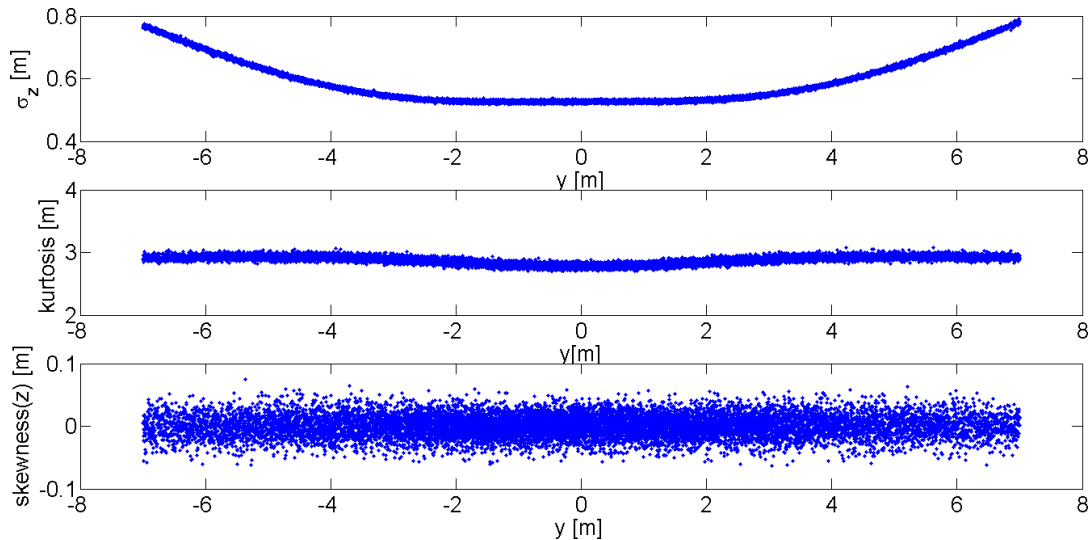


Figure 5: analysis of the derived statistical moments of for k-TLS profile using 100.000 MC – standard deviations, kurtosis and skewness.

The B-spline approximation has been recomputed by means of the assumed refined propagated scholastic observations according to classical and MO GUM.

Figure 6 shows a small sequence of the entire results of the approximated bridge underside of the carriageway. The TLS point cloud are represented in green. The results of the B-Spline using different variance covariance matrices (VCMs) for the stochastic model (refer to Sec. 3) are highlighted in red for the identity VCM (identical variances for all observations and stochastically independent), blue for the VCS, performed by means of the classical GUM, and black for the VCS, gained by means of the Monte Carlo simulation. Only small deviations among the three curves can be detected.

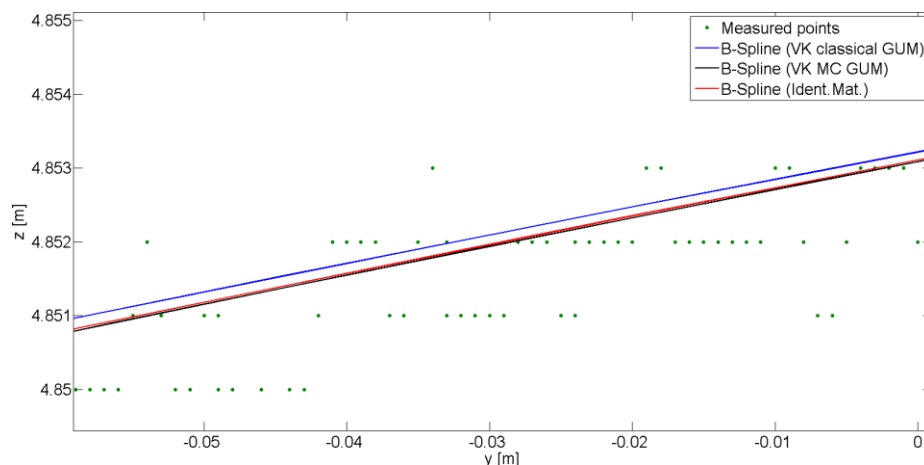


Figure 6: Comparison between computed uncertainties using classical GUM (black) and Monte Carlo GUM (gray).

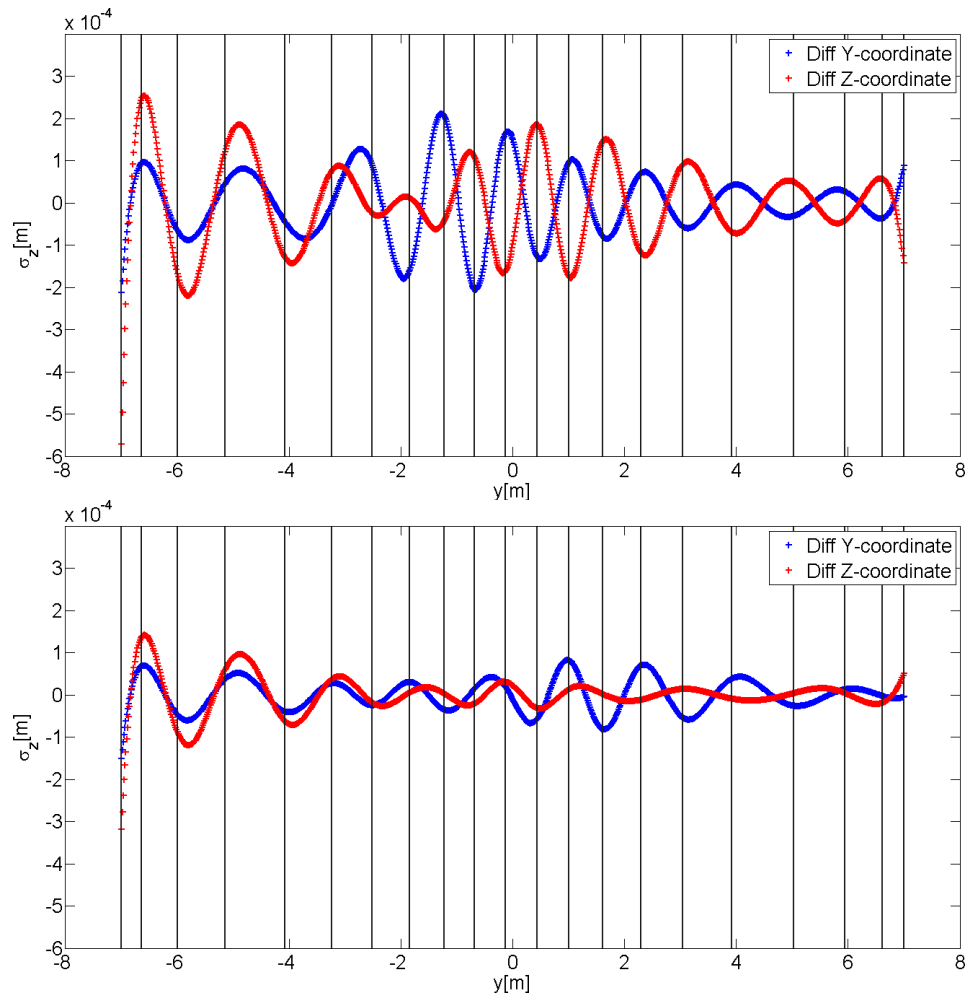


Figure 7: Difference between estimated Y- and Z-coordinate for the approximated curves (B-Spline) with and without VCMs information: top using classical GUM, bottom using Monte Carlo simulation.

Figure 7 (top) shows differences of equally weighted estimated observations and unequal stochastic observations according to classical GUM, here for both estimated observations (Y- and Z-coordinate). Figure 7 (bottom) represents the differences of equally weighted estimated observations and unequal stochastic observations according to MC-GUM approach. The vertical black lines in both subfigures shows the positions of the control points. The remaining trend of both parts can be interpreted as a harmonic oscillation. The most maxima of the remaining amplitudes are located near the control points and are affected strongly by its selection. Differences are of magnitude of about 0.6 - 0.7 mm for classical GUM and 0.5 - 0.7 mm for MC approach.

## 5. CONCLUSIONS

The presented two methods, classical GUM and Monte Carlo GUM, provide a priori variance-covariance-matrix for the spatial approximation of the TLS profile. The stochastic models have been implemented successfully. The differences in the residuals of both methods after the spatial approximation compared to each other shows negligibly varieties. Nonetheless, the Monte Carlo method includes different distribution functions for the

influence parameters and is consequently more flexible for further investigations. The difference between the residuals after the approximation with and without stochastic information are in the range of  $\pm 0,5$  mm, which is twice as big as the accuracy of the approximation. The complete reduction of the systematic errors in the residuals by the use of a stochastic model needs more investigation. The differences between estimated coordinate for the approximated curves (B-Spline) with and without VCMs information still have an oscillation, which results from the choice of control points. Furthermore, the influence of the spatial approximation by changing the parameters, like the degree or the number of basic functions, to the resulting residuals is larger than the influence of changing the stochastic model.

## REFERENCES

Alkhatib, H., Neumann, I., Kutterer, H. (2009): *Uncertainty modeling of random and systematic errors by means of Monte Carlo and Fuzzy techniques*. Journal of Applied Geodesy, Vol. 3, 67-80.

Alkhatib, H.; Kutterer, H. (2013): *Estimation of Measurement Uncertainty of kinematic TLS Observation Process by means of Monte-Carlo Methods*, In: Journal of Applied Geodesy, Jg. 7, Nr. 2/2013, S. 125–134.

De Boor, C. (1989): *On calculating with B-splines*, Jour. Approx. theory, vol. 6, pp. 121-128.  
Hansen M., von der Haar C., Marx S. (2012): *Assessment of heavy load vehicles without disability of traffic*, Proceedings of the 8th Central European Congress on Concrete Engineering (CCC 2012), Plitvicer Seen, Kroatien, 4.-6. Oktober 2012, pp. 169 – 174.

Heunecke, O., Kuhlmann, H., Welsch, W., Eichhorn, A., Neuner, H. (2013): *Handbuch geodätischer Überwachungsmessungen*, 2nd ed., Wichmann Verlag, Heidelberg.  
ISO (1995): *Guide to the Expression of Uncertainty in Measurement (GUM)*. International Organization of Standardization, Geneva / Switzerland.

ISO (2007): *Evaluation of Measurement Data – Supplement I to the GUM – Propagation of Distribution using a Monte-Carlo Method*. Joint Committee for Guides in Metrology, Bureau International des Poids et Mesures. JCGM 101.

Kutterer, H.; Alkhatib, H.; Paffenholz, J.-A.; Vennegeerts, H. (2010): *Monte-Carlo Simulation of Profile Scans from Kinematic TLS*, In: FIG (Hg.): Proceedings of the XXIV FIG Congress. Facing the Challenges - Building the Capacity. Sydney, Australia, 11.-16.04.2010.

Kutterer, H.; Paffenholz, J.-A. und Vennegeerts, H. (2009): *Kinematisches terrestrisches Laserscanning*, Zeitschrift für Geodäsie, Geoinformation und Landmanagement (zfv), vol. 134, Wißner-Verlag, Augsburg, pp. 79-87.

Liebig, J. P.; Grünberg, J.; Paffenholz, J.-A. & Vennegeerts, H. (2011): *Taktile und laserbasierte Messverfahren für die messtechnische Überwachung einer Autobahnbrücke*. In: Bautechnik 88 (11), S. 749–756. DOI: 10.1002/bate.201101514.

Neuner H., Schmitt C., Neumann I. (2013): *Modelling of terrestrial laser-scanning profile measurements with free-form elements*, In: Proceedings of the 2nd Joint international Symposium on Deformation Monitoring. Nottingham, England.

NTH-BAU (2010): *Life Cycle Engineering for Engineering Structures and Buildings - Strategies and Methods*, Topic 6: Application of life cycle concepts to civil engineering structures, 2010-2013, www.nth-bau.de.

Paffenholz, J.-A., Vennegeerts, H., Kutterer, H. (2008): High frequency terrestrial laser scans for monitoring kinematic processes. CD-ROM Proc. INGENEO 2008, Bratislava / Slovakia.

Piegel L., Tiller W. (1997): *The Nurbs Book*, Springer-Verlag, Berlin Heidelberg, 2nd ed., ISBN 9783540615453.

Schmitt C., Neuner H., Neumann I. (2013): *Strain detection on bridge constructions with kinematic laser scanning*, In: Proceedings of the 2nd Joint international Symposium on Deformation Monitoring. Nottingham, England.

ZÖLLER+FRÖHLICH (2007): *Spezifikationen Imager 5006*, Zoller+Fröhlich GmbH, 2007, Wangen – Germany.

## BIOGRAPHICAL NOTES

**Dr. Hamza Alkhatib** received his Dipl.-Ing. in Geodesy and Geoinformatics at the University of Karlsruhe in 2001 and his Ph.D. in Geodesy and Geoinformatics at the University of Bonn in 2007. Since 2007 he has been postdoctoral fellow at the Geodetic Institute at the Leibniz Universität Hannover. His main research interests are: Bayesian Statistics, Monte Carlo Simulation, Modeling of Measurement Uncertainty, Filtering and Prediction in State Space Models, and Gravity Field Recovery via Satellite Geodesy.

**M. Sc. Claudius Schmitt:** received his M.Sc. in Geoinformatics and Surveying at the University of Applied Science in Mainz in 2011. Since then he has been a research assistant at the Geodetic Institute at the Leibniz University Hannover and moved 2014 to the engineering geodesy research Group of Univ.Prof.Dr.-Ing. Neuner at the Vienna University of Technology. His research topics are the provision of the geometry for Finite Element Methods by spatial surface approximation of 3D measured point clouds.

**Prof. Dr. Ingo Neumann** received his Dipl.-Ing. and Ph.D. in Geodesy and Geoinformatics at the Leibniz Universität Hannover in 2005 and 2009, respectively. Since 2012 he has been a Full Professor at the Geodetic Institute of the Leibniz Universität Hannover. His research areas are: adjustment theory and error models, quality assessment, geodetic monitoring, terrestrial laser scanning, multi sensor systems, and automation of measurement processes. He is active in national and international scientific associations. He is a member in various commissions and organizations, as the German Society of Surveying, the Society for Calibration of Geodetic

Devices, and the German Institute of Standardization.

## CONTACTS

Dr. Ing. Hamza Alkhatib and Prof. Dr. Ingo Neumann  
Leibniz Universität Hannover  
Geodetic Institute  
Nienburger Str. 1  
30966 Hannover  
Germany  
Tel. +49 511 762-2464  
Fax +49 511 762-2468  
Email: {alkhatib,neumann}@gih.uni-hannover.de  
Web site: <http://www.gih.uni-hannover.de>

Claudius Schmitt, M.Sc.  
Vienna University of Technology  
Department of Geodesy and Geoinformation  
Research Group Engineering Geodesy  
Gußhausstraße 27-29  
1040 Wien  
Austria  
Tel. +43 1 58801 12843  
Fax + 43 1 58801 12894  
Email: [claudius.schmitt@geo.tuwien.ac.at](mailto:claudius.schmitt@geo.tuwien.ac.at)  
Web site: [geo.tuwien.ac.at](http://geo.tuwien.ac.at)